

Field and frequency dependence of charge-density-wave conduction in NbSe₃

G. Grüner, A. Zettl, and W. G. Clark

Department of Physics, University of California, Los Angeles, California 90024

John Bardeen

Department of Physics, University of Illinois at Urbana-Champaign, Urbana, Illinois 61801

(Received 22 June 1981)

Frequency (ω)- and field (E)-dependent conductivity (σ) measurements are reported in both charge-density-wave (CDW) states of the linear-chain compound NbSe₃. There is a direct scaling between the observed E and ω dependence for parameters corresponding to $E > 2E_T$, where E_T is the threshold field for the onset of nonlinear conductivity. The functional form of $\sigma(E)$ is in agreement with a tunneling model. In contrast to the threshold field, there is no threshold frequency for the onset of frequency-dependent conductivity. This is accounted for by a contribution to $\sigma(\omega)$ from the excitation of oscillations of the pinned CDW at low frequencies. Experiments involving the combined application of dc and ac fields $V = V_0 + V_1 \cos \omega t$ do not show evidence for photon-assisted tunneling, and only the classical limits of the tunneling formalism are observed. We discuss these observations and suggest reasons for the absence of quantum effects when both ac and dc fields are present. Various models of CDW transport are compared.

I. INTRODUCTION

It has recently been shown experimentally that several unusual electrical transport phenomena occur in NbSe₃ due to the motion of charge density waves (CDW) which are pinned at a low electric field, but which become mobile above a threshold field E_T . These properties include nonlinear dc conduction with a threshold,¹ a strongly frequency-dependent electrical conductivity,² the generation of narrow-band and wide-band noise,^{1,3} enhancement of the dc conductivity by a large amplitude electric field,⁴ and increased pinning of the CDW with the introduction of impurities.⁵ They have been observed both in the high-temperature CDW phase, between $T_1 = 149$ K and $T_2 = 59$ K, where only one incommensurate CDW is present, and in the low-temperature $T < T_2$ phase where two incommensurate CDW's exist. Some of these properties have also just been reported for TaS₃ in which the CDW's are commensurate.⁶

Various microscopic theories have been proposed⁷⁻⁹ to explain these observations; two of them describe the frequency- and field-dependent conductivity in detail. One of them is a quantum-mechanical tunneling model by Bardeen⁸ and the other is a classical model of CDW pinning in a periodic potential by Grüner, Zawadowski, and

Chaikin.⁹

In this communication we report careful measurements of the conductivity σ in the CDW state as a function of an applied dc electric field of amplitude E and a small amplitude ac field of frequency ω . Both the dc and ac response to these excitations have been measured. We denote them as $\sigma_{dc}(\omega, E)$ and $\sigma_{\omega}(\omega, E)$, where the subscript refers to the frequency at which the response is measured and the quantities in parenthesis indicate the nature of the driving forces applied to the sample. Although we have measured both the real and imaginary parts of σ , in this paper we report only our experimental results for its real part. For simplicity, in what follows it is to be understood that σ stands for only the real part, except when an imaginary part is indicated explicitly. Throughout σ_{dc} is defined to be $[I(E) - I(0)]/E$ rather than dI/dE .

The motivation for our work was to test two predictions of the tunneling model⁸ and to explore the applicability of both the classical and tunneling models for CDW motion. One of our main experimental results is that for $E > 2E_T$, there is a *direct scaling* between E and ω for CDW conduction in NbSe₃; i.e., $\sigma_{dc}(0, E) = \sigma_{\omega}(\omega, 0)$. This behavior is predicted by the tunneling model. A second result is that for E closer to (and on either side of) E_T , $\sigma_{\omega}(\omega, 0) > \sigma_{dc}(0, E)$ and, in contrast to $\sigma_{dc}(0, E)$,

there is no threshold for $\sigma_\omega(\omega, E)$. This disagrees with the tunneling model taken by itself, but can be well accounted for if, in addition to the tunneling current, a phenomenological internal excitation of the pinned CDW is considered. The latter contribution becomes more prominent as T is lowered. Another major experimental result is that the joint application of a dc field below E_T and an ac field does not produce the photon-assisted tunneling predicted by the tunneling model.

Several other related points are also considered in this paper. The relationship of the classical model to the experimental results and the tunneling model are discussed. The tunneling model is based on a semiconductor model for the CDW's and Tucker's¹⁰ theory for superconductor-insulator-superconductor (SIS) tunnel junctions. Although it works quite well when only a dc or an ac excitation is used, it appears to be inadequate when both are present, and requires further development. Possible reasons for this difficulty are discussed.

This paper is organized as follows. In Sec. II we summarize the two models which have been proposed to account for $\sigma_{dc}(0, E)$ and $\sigma_\omega(\omega, 0)$, together with the predictions of these models concerning experiments in which dc and ac excitations are applied jointly. Section III presents the experimental details and results. They are discussed in Sec. IV, along with several unresolved problems. Finally, a review of the basis for the classical and quantum tunneling models for depinning is given in the Appendix. An unpinned incommensurate CDW can move through the lattice in response to applied electric field and carry electrons with it. There is no energy gap to be overcome for flow by electrons condensed in the CDW, although one is required for current carried by soliton or quasiparticle excitations. It is found experimentally that at high electric fields or at high frequencies, CDW's become depinned. The limiting conductivity is in both cases about what one would expect in the absence of the CDW's. Motion of unpinned CDW's on the basis of a simple model discussed in the Appendix makes this result plausible.

II. THEORETICAL MODELS

The two models which have been developed for a detailed comparison with the wide variety of phenomena associated with the electrical transport properties of moving CDW's are the classical⁹ and the quantum-mechanical tunneling⁸ models. In this section we summarize their main features.

As discussed in the Appendix, the motion of CDW's can be described in terms of the phase (ϕ) of the wave

$$\phi = 2k_F(x - v_d t) + \phi_1(x, t), \quad (2.1)$$

where k_F is the one-dimensional (1D) Fermi wave vector and v_d is the phase velocity of the wave. For a pinned wave, $v_d = 0$ and ϕ_1 , a slowly varying function of x , is a solution of [see (A11)]

$$\frac{d^2\phi_1}{dt^2} + \Gamma \frac{d\phi_1}{d\tau} + \omega_p^2 V'(\phi_1) = \beta E(t), \quad (2.2)$$

where the second term represents damping, $V'(\phi_1)$ is the gradient of a periodic pinning potential, $V(\phi_1)$, such that $V'(\phi_1) \rightarrow \phi_1$ when ϕ_1 is small, ω_p is the pinning frequency, $E(t)$ is the applied electric field, and $\beta = 2k_F e / (m + M_F)$, where M_F is the Fröhlich mass associated with motion of the ions and m is the band mass of the electrons.

In the classical pinning potential model,⁹ $\sigma_\omega(\omega, 0)$ at low ac fields is determined by Eq. (2.2), and the experimental results suggest the response is that of an overdamped oscillator. Consequently, the first term on the left of Eq. (2.2) is neglected. The response to a small ac voltage whose amplitude V_1 is much less than the threshold voltage V_T is then given by⁹

$$\sigma_\omega(\omega, 0) = \sigma_\omega(\infty, 0) \frac{\omega^2}{\omega^2 + \omega_p^4 / \Gamma^2}, \quad (2.3)$$

where $\sigma_\omega(\infty, 0)$ is the conductivity at frequencies much higher than ω_p^2 / Γ .

In a dc field the periodic pinning potential is tilted by the electric field, so the system may be regarded as particles moving down a staircase potential. There is no dc current until the potential peaks are sufficiently reduced by the field so that the barrier can be overcome by the potential drop. The particles accelerate, and slow down during the motion. This leads to a natural explanation of the observed narrow-band noise.^{1,3} The model also leads to a sharp increase of the conductivity above E_T , and the differential conductance dI/dV diverges at E_T ,¹¹ in contrast to the observations which show a smooth increase of dI/dV above E_T .¹¹ To account for the observed gradual rise in conductivity above threshold it is necessary to assume an appropriate distribution of pinning energies.¹² The observation of well defined narrow-band noise peaks^{1,3} however suggest that such a distribution is not important in NbSe₃.

According to the tunneling model,⁸ particles can tunnel through the potential barriers when the field

is less than that required for the particles to surmount the potential peaks by classical motion. To calculate the tunneling current, a semiconductor model with a gap energy ϵ_g equal to the energy $\hbar\omega_p$ was used, and the tunneling probability was determined from the theory for Zener tunneling.⁸ The relationship between the classical phase model and the semiconductor model is discussed in the Appendix.

To account for the threshold field, it was assumed that there is a correlation length L for the CDW across which the field must be applied to be effective in accelerating the wave. The correlation length is presumably twice the mean free path of electrons.⁸ In a dc field E , the tunneling probability is given by an expression of the form

$$P(E) = [1 - (E_T/E)] \exp(-E_0/E). \quad (2.4)$$

The parameter E_0 is related to ϵ_g by the usual Zener expression $E_0 = \pi\epsilon_g^2/4\hbar e^* v_F$, where the effective charge $e^* = me/(m + M_F)$ and v_F is the Fermi velocity. The threshold field is given by $e^* E_T L = \epsilon_g$. Upon introduction of the coherence length $\xi_0 = 2\hbar v_F/\pi\epsilon_g$ analogous to that of superconductors, the relation $E_0 = E_T(L/2\xi_0)$ is obtained. This relation applies only when $L \gg 2\xi_0$. When $L \ll 2\xi_0$, $E_0 = E_T$ and in general $E_0 = E_T[1 + (L/2\xi_0)]$. At temperatures close to the transition temperature T_p , E_0 is enhanced by the factor n/n_c , where n_c is the concentration of electrons condensed in the CDW.

A theory developed by Tucker¹⁰ for the quantum limit of the tunneling current in superconductor-insulator-superconductor (SIS) tunnel junctions was used to account for the frequency dependence of the current. The voltage across the correlation length, L , replaces the voltage across the SIS junction and e^* replaces e . It is only in the replacement of e by e^* that the CDW is included in the model.

Tucker's theory leads to the following expressions for the ac current $I_1(\omega) \cos\omega t$ and the change in dc current, ΔI_{dc} , resulting from an applied voltage $V_0 + V_1 \cos\omega t$. When $V_1 \ll V_0$

$$\begin{aligned} I_1(\omega) &= (e^* V_1 / 2\hbar\omega) [I_0(V_0 + \hbar\omega/e^*) \\ &\quad - I_0(V_0 - \hbar\omega/e^*)], \\ \Delta I_{dc} &= (e^* V_1 / 2\hbar\omega)^2 [I_0(V_0 + \hbar\omega/e^*) - 2I_0(V_0) \\ &\quad + I_0(V_0 - \hbar\omega/e^*)]. \quad (2.6) \end{aligned}$$

Here $I_0(V)$ is the dc current for an applied dc voltage V . For small $\hbar\omega/e^*$, these reduce to the classical expressions,

$$I_1(\omega) = V_1 (dI/dV)_{V_0},$$

$$\Delta I_{dc} = (V_1^2/4) (d^2I/dV^2)_{V_0}.$$

For $V_0 = 0$, (2.5) gives the following simple relation for the tunneling contribution (σ^f) to the ac conductivity:

$$\sigma^f(\omega, 0) = \sigma^f(0, E), \quad (2.7)$$

with $\hbar\omega = e^* L E$. For dc voltages, σ^f is defined to be I/E . At threshold, the energy $\hbar\omega_T = e^* L E_T$ is the energy gap $\hbar\omega_p$. Thus, the tunneling model predicts that there is a scaling relation between the field and frequency-dependent conductivity, with the relation $\hbar\omega_T = e^* L E_T$.

Another important prediction of Eq. (2.5) is that a finite dc CDW current is obtained under a combined dc and ac excitation for which the peak amplitude is less than the threshold, $V_0 + V_1 < V_T$, but whose frequency is large enough to span the difference between V_1 and V_T : $V_1 + \hbar\omega/e^* > V_T$. In particular, for small V_1 , and $V_0 - \hbar\omega/e^* < V_T < V_0 + \hbar\omega/e^*$, Eq. (2.6) gives

$$\Delta I_{dc} = (e^* V_1 / 2\hbar\omega)^2 I_0(V_0 + \hbar\omega/e^*)$$

since the last two terms in (2.6) are zero below the CDW threshold. This results predicts that the energy quantum $\hbar\omega/e^*$ can span the difference between V_0 and V_T , even though the classical field amplitude V_1 is too small to do so. Thus the tunneling model predicts there should be photon-assisted tunneling of the CDWs.

In comparison, the classical model⁹ does not predict the exact scaling of Eq. (2.7). The relation between $\sigma_\omega(\omega, 0)$ and $\sigma_{dc}(0, E)$ obtained with it depends somewhat on the spatial form used for the pinning potential. Those which have been used⁹ exhibit a qualitatively similar behavior for $\sigma_\omega(\omega, 0)$ and $\sigma_{dc}(0, E)$ but not exact scaling. Another difference is that the classical model does not predict photon-assisted tunneling. The ac voltage acts only as a time varying driving force, and the only dc component to the CDW current is due to the average motion which occurs when the instantaneous total voltage $V_0 + V_1$ exceeds V_T .

III. EXPERIMENTAL DETAILS AND RESULTS

The NbSe₃ samples used in this work were provided by N. P. Ong (USC) and by R. M. Fleming (Bell Laboratories, abbreviated BL). The BL samples have a large resistivity ratio, and consequently

lower threshold fields for nonlinear conduction than the USC samples if $\sigma_{dc}(0,E)$ is measured at the same temperature. The USC samples are from the same batch used earlier for our investigations of $\sigma_{\omega}(\omega,0)^2$ and narrow-band noise.³ In the present work $\sigma_{dc}(0,E)$ was measured using both continuous and pulse methods to avoid self-heating of the sample at high E . A comparison of $\sigma_{dc}(0,E)$ measured by the two methods showed that self-heating is negligible up to $E \sim 5E_T$, even for continuous application of the field. The quantity $\sigma_{\omega}(\omega,0)$ was measured up to $\omega/2\pi$ as high as 1 GHz using an H. P. 8754 A network analyzer. The condition $V_1 < 0.1V_T$ was always satisfied. Measurements with various values of V_1 down to $V_1 = 0.01V_T$ did not reveal any dependence of $\sigma_{\omega}(\omega,0)$ on V_1 . We therefore believe our results accurately represent the quantity $\sigma_{\omega}(\omega,0)$.

The experiments to measure $\sigma_{dc}(\omega,E)$ with the joint application of dc and ac voltages (ac-dc coupling) were performed using radio-frequency circuits developed for that purpose in our laboratory.

Typical uncertainties in our measurements of σ are reflected in the scatter of the data or error flags. The temperature was provided by a helium gas flow system constructed in our laboratory. Its stability was about 0.1 K and its accuracy was about 1 K. The conductivity was measured using a two-probe configuration with a lead spacing usually less than 1 mm and contact resistances which were usually two orders of magnitude smaller than the sample resistance. It is important for this work that we have avoided uncertainties associated with variations in sample properties by making all electrical measurements on the same sample during the same experimental run. Also, the short samples used reduce the likelihood of inhomogeneous strains which develop in the sample. Care has also been exercised to avoid spurious field dependences from nonuniform sample cross sections, contact effects, etc. We have performed the ac and dc measurements on several samples at various temperatures both in the high-temperature and in the low-temperature CDW phase. In this communication we report our observations only at selected temperatures. Measurements at other temperatures lead to the same observations, with the only difference being due to the temperature dependence of the parameters involved in the analysis of the experimental data.

In Fig. 1 we show $\sigma_{dc}(0,E)$ and $\sigma_{\omega}(\omega,0)$ measured in the upper CDW state at $T = 130$ K over a broad range of E (upper axis) and ω (lower axis).

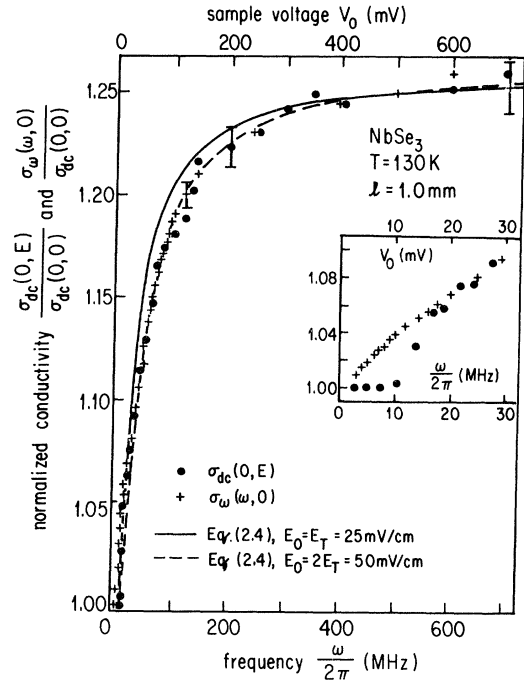


FIG. 1. Normalized ac and dc conductivity as a function of ω (lower scale) and V_0 (upper scale) in NbSe_3 at $T = 130$ K (upper CDW state). The ω scale has been adjusted to demonstrate the scaling observed for $V_0 > 2V_T$ and predicted by the tunneling model [Eq. (2.4)]. The dashed line, corresponding to $E_0 = 2E_T$ gives a better fit to the tunneling model than $E_0 = E_T$ (solid line). The inset shows that $\sigma_{\omega}(\omega,0) > \sigma_{dc}(0,E)$ near V_T , and suggests that internal excitations [Eq. (4.2)] are important near V_T .

The correspondence between E and V is made using the distance $l = 1.0 \pm 0.1$ mm between the electrical contacts to the sample. In Fig. 2, similar measurements performed below T_2 , on a USC sample are displayed. The most important feature of Figs. 1 and 2 is, that by a suitable scaling of ω and E , both results overlap over most of the range covered, as predicted by the tunneling model [see Eq. (2.7)].

The data for small ω and E , shown in detail in the inserts of Figs. 1 and 2 indicate that a sharp threshold for the onset of dc nonlinearity field is not accompanied by a corresponding sharp threshold frequency ω_T . Instead the ω dependence extends to $\omega \rightarrow 0$ for both measurements. This feature is shown more strikingly in Fig. 3, where experiments performed at $T = 32$ K are displayed. Owing to the lower temperature, both the field and frequency dependence move to higher E and ω , and the behavior near to E_T is more clearly ob-

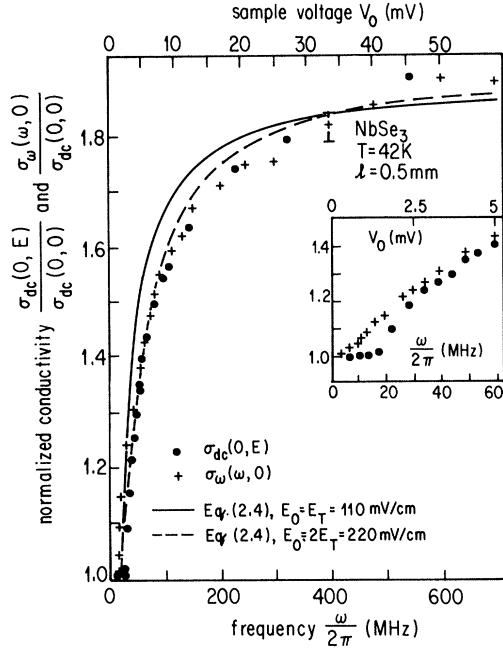


FIG. 2. Normalized ac and dc conductivity as a function of ω (lower scale) and V_0 (upper scale) in NbSe_3 at $T=42$ K (lower CDW state). The ω scale has been adjusted to demonstrate the scaling observed for $V_0 > 2V_T$ and predicted by the tunneling model [Eq. (2.4)]. The dashed line, corresponding to $E_0 = 2E_T$ gives a better fit to the tunneling model than $E_0 = E_T$ (solid line). The inset shows that $\sigma_\omega(\omega, 0) > \sigma_{dc}(0, E)$ near V_T , and suggests that internal excitations [Eq. (4.2)] are important near V_T .

served. By comparing the overall field and frequency dependence measured up to 1 GHz and field values much higher than shown in the figure, a scaling of the ω and E dependence (in a way similar to that shown in Fig. 1) gives a correspondence between V_0 and ω . This leads to the assignment $\omega_T/2\pi = 113$ MHz at $T=32$ K. A sharp threshold field is seen for $\sigma_{dc}(0, E)$ at $V_T = 14$ mV, but the variation with ω extends down to $\omega \rightarrow 0$.

Next we discuss our experiments which involve the joint application of ac and dc fields. Equations (2.5) and (2.6) also predict a change in σ when dc and ac fields are applied simultaneously to the sample, and suggest the possibility of detecting a dc current in the presence of a high-frequency excitation. We have searched for both in an attempt to verify (2.5) and (2.6).

In both equations the dc field V_0 and frequency $\omega/2\pi$ appear in the combination $V_0 + \hbar\omega/e^*$ or $V_0 - \hbar\omega/e^*$. We have in all cases first established the scaling relations between V_0 and $\hbar\omega/e^*$ by measuring the field and frequency dependence

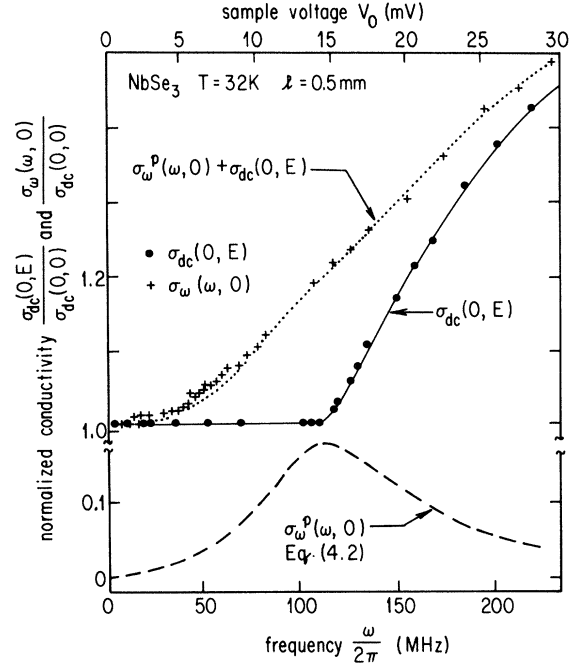


FIG. 3. Normalized ac and dc conductivity as a function of ω (lower scale) and V_0 (upper scale) in NbSe_3 at $T=32$ K (lower CDW state). The ω scale has been adjusted by scaling at values of ω beyond the range graphed. Addition of the proposed internal excitation contribution $\sigma_\omega^p(\omega, 0)$ [dashed line, Eq. (4.2)] to the tunneling part $\sigma_{dc}(0, E)$ (solid line) gives the dotted line, which provides a good fit to $\sigma_\omega(\omega, 0)$.

separately before performing the experiments with joint ac and dc excitation. Plots similar to Figs. 1 and 2 were used to arrive at the correspondence between V_0 and $\hbar\omega/e^*$. Measurements on various samples with different lengths l established that the observed frequency dependence is independent of l . The threshold field V_T is inversely proportional to l , so that E_T is constant as expected. All ac-dc coupling experiments were performed at $T=42$ K where the measured V_T corresponds to 113 MHz as established before, on the sample shown in Fig. 3. In the first experiment we measured $\sigma_\omega(\omega, E)$ at two different frequencies in the presence of a dc bias of varying amplitude. Figure 4 shows $\sigma_\omega(\omega, E)$ at 30 MHz and at 80 MHz as a function of V_0 . In this experiment, $V_1 = 2$ mV peak, which is much smaller than V_T . Therefore, the series expansion in powers of V_1 used to obtain Eq. (2.5) is appropriate. From Fig. 4 it is seen that as ω decreases, the threshold becomes progressively less distinct and shifts to lower V_0 .

The results of our search for photon-assisted tun-

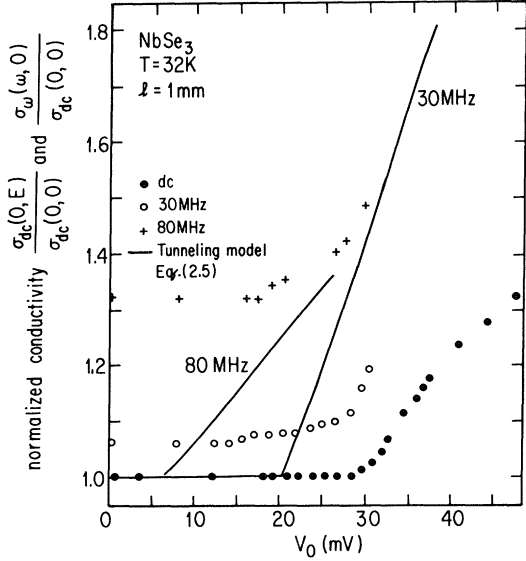


FIG. 4. Normalized dc and ac conductivity (30 and 80 MHz) as a function of V_0 in NbSe_3 at $T=32$ K. The solid lines are the prediction of the tunneling model [Eq. (2.5)].

neling in NbSe_3 are shown in Fig. 5. In these experiments ΔI_{dc} is measured while applying a V_0 somewhat below V_T and a low-amplitude ac voltage over a wide range of ω , and plotted in terms of σ . The solid dots show the usual threshold behavior of $\sigma_{\text{dc}}(0, E)$ with no rf excitation applied for the same sample and run as presented in Fig. 3.

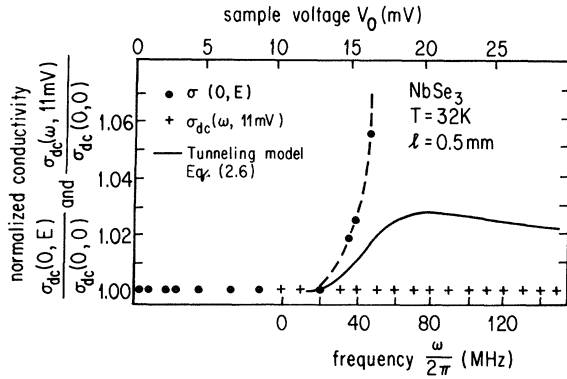


FIG. 5. Normalized dc conductivity as a function of V_0 only (upper scale) and as a function of a combined dc ($V_0=11$ mV) and ac ($V_1=2$ mV peak, ω variable) excitations. The frequency is added to $V_0=11$ mV on the lower scale using the scaling relation established for this sample. The solid line shows the photon-assisted tunneling predicted by Eq. (2.6), which is not observed experimentally (crosses). The dashed line is a guide to the eye for $\sigma_{\text{dc}}(0, E)$.

The crosses indicate $\sigma_{\omega}(\omega, V_0=11$ mV) with an ac excitation of amplitude $V_1=2$ mV peak applied in the range $0 < \omega/2\pi < 150$ MHz. The frequency is added to the V_0 axis starting at 11 mV using the frequency-voltage scaling relation $V/\omega=13$ mV/226 MHz established for this sample in Fig. 3. As $V_0+(h\omega/e^*)$ defined in this manner extends beyond V_T , within our experimental resolution there is no increase whatsoever in σ_{dc} .

IV. INTERPRETATION

In this section, we interpret the experiments described in the preceding section in terms of the tunneling and, to a lesser extent, the classical model. The discussion divides naturally into the three headings listed below.

A. Field-frequency scaling, $E > 2E_T$

First we consider the scaling between ω and E for $E > 2E_T$, as shown in Figs. 1 and 2. It is clear that the scaling expressed by Eq. (2.7) describes the experiments. The same situation has also been observed in TaS_3 . Hence, this prediction of the tunneling model is well satisfied by our experiments.

A more detailed comparison with Eq. (2.4) of the tunneling model is indicated by the solid and dashed lines in Figs. 1 and 2. Two parameters are adjusted to make the fits. First, the amplitude of the CDW term in the model is set to make $\sigma_{\text{dc}}(0, E)/\sigma_{\text{dc}}(0, 0)$ coincide with the experimental value at the ratio 1.25 in Fig. 1 (130 K) and 1.85 in Fig. 2 (42 K). Then, two values of E_0 are considered, $E_0=E_T$ (solid line) and $E_0=2E_T$ (dashed line). It is seen that the data fall fairly close to the detailed form given by (2.4). The assignment $E_0=2E_T$ gives a better fit to the experimental data, both at the upper and at the lower transition, than the assignment $E_0=E_T$. In all cases, E_T has been determined from the measured threshold in $\sigma_{\text{dc}}(0, E)$.

Since we obtain the same overall behavior both at the higher and at the lower CDW phase, we conclude that the presence of the two CDW's below T_2 does not play an important role at these frequencies and fields. Indeed, the depinning of the second CDW below T_2 occurs at electric fields higher than those shown in Fig. 2, and consequently we expect an ω -dependent response due to the second CDW to play an important role only at

higher frequencies.

It is noteworthy that as long as T is not too close to the Peierls transition temperature (T_p), $E_0 = 2E_T$ fits the data in NbSe₃ over a very wide range of temperature and E_T . The same type of behavior also has been observed⁶ for TaS₃, but with $E_0 = 5E_T$ and E_0 approximately constant from 150 to 200 K. In both CDW phases of NbSe₃, E_0 increases as $T \rightarrow T_p$, while the fraction of electrons condensed in the wave, n_c/n , decreases to zero at T_p . For the data used in Ref. 8, the best fit is obtained for $E_0 = E_T$ for the lower CDW phase.

The tunneling model provides a good fit to the experiments discussed here. As mentioned in Sec. II, the classical model gives an approximate scaling between ω and E , but not the extremely close scaling seen in our experiments and predicted by the tunneling model.

It is worth noting that the frequency associated with the scaling is not the same as that associated with narrow-band noise (Ω). This is evident, for example, from the fact that Ω does not exhibit the scaling seen for ω . As indicated by experiments and the classical model, Ω is proportional to the CDW current.

We finish this section by presenting the parameters which characterize the dc and ac response of the CDW's in NbSe₃ at several temperatures. They are summarized in Table I. The threshold frequency is obtained from the scaling shown in Figs. 1–3.

The length ϵ_g/e^*E_T should correspond to L . The estimates given in the table are obtained by taking $e^*/e = 10^{-3}$. The values of $2\xi_0$ are obtained from $4\hbar v_F/\pi\epsilon_g$, with $v_F = 10^7$ cm/sec. From the discussion below Eq. (2.4), E_0/E_T should be $(n/n_c)[1 + (L/2\xi_0)]$. Thus the observed ratio $E_0/E_T = 2$ is not unreasonable for $T = 42$ K and

$T = 32$ K, particularly since the fraction of condensed electrons may be somewhat less than unity at the higher temperature. The value $2E_T$ for the upper transition at $T = 130$ K also probably arises both from the factor n/n_c and perhaps a smaller value for e^*/e than assumed.

B. Response close to E_T

For $E < 2E_T$, Figs. 1–3 indicate an apparent disagreement between our experimental results and the scaling predicted in Eq. (2.7) using the tunneling model. We suggest that the observed increase of $\sigma_\omega(\omega, 0)$ above $\sigma_{dc}(0, E)$ is caused by another contribution (σ^p) which should be added to the tunneling part (σ^t). The latter applies to displacement of the CDW as a whole. The other contribution corresponds to an excitation of oscillations of the pinned CDW centered around the pinning frequency, $\omega_p = \omega_T$.

From Eq. (2.1) and the usual phenomenological model^{13,14} [Appendix (A11)] it follows that the contribution to the complex dielectric function ϵ_p from the pinned mode, is

$$\epsilon^p(\omega) = \frac{\Omega_p^2}{\omega_T^2 - \omega^2 - i\Gamma\omega}, \quad (4.1)$$

where Ω_p^2 is a measure of the oscillator strength.

Expression (4.1) without the damping term was also used by Lee, Rice, and Anderson¹⁵ to describe a pinned CDW mode. The corresponding contribution to the complex conductivity is

$$\sigma^p(\omega) = \sigma^p(\omega_T) \left[\frac{\Gamma^2\omega^2}{(\omega_T^2 - \omega^2)^2 + \Gamma^2\omega^2} - \frac{i\Gamma\omega(\omega_T^2 - \omega^2)}{(\omega_T^2 - \omega^2)^2 + \Gamma^2\omega^2} \right]. \quad (4.2)$$

TABLE I. CDW parameters of NbSe₃ obtained from the conductivity measurements and scaling relations shown in Figs. 1–3.

Temperatures T (K)	Threshold voltage V_T (mV)	Contact spacing l (mm)	Threshold field E_T (mV/cm)	$\omega_T/2\pi$ (MHz)	$\hbar\omega_T = \epsilon_g$ (10^{-20} erg)	$L = \epsilon_g/e^*E_T^a$ (μm)	$2\xi_0^b$ (μm)
130	11	1.0	110	11	7.4	5	150
42	1.25	0.5	25	14.5	9.7	19	120
32	14	0.5	280	113	76	17	16

^aUsing $e^*/e = m/(m + M_F)1 = 10^{-3}$.

^bFrom $2\xi_0 = 4\hbar v_F/\pi\epsilon_g$ with $v_F = 10^7$ cm/sec.

While one would not expect the two contributions to be additive when $\omega \gg \omega_T$, it should be a good approximation in the neighborhood of ω_T where the tunneling current is small. Thus, in this region, Eq. (2.7) is modified to read

$$\sigma_\omega(\omega, 0) = \sigma_{dc}^t(0, E) + \sigma_\omega^p(\omega, 0), \quad (4.3)$$

where the tunneling contribution $\sigma_{dc}^t(0, E)$ is obtained using the scaling relation established at high E and ω . In Fig. 3 we have fitted $\sigma_\omega(\omega, 0)$ to Eq. (4.3) with $\sigma_{dc}^t(0, E)$ as given by the observed field dependence, shown by the solid circles and solid line in Fig. 3, and $\sigma_\omega^p(\omega, 0)$ given by Eq. (4.2), with the parameters ω_T and Γ adjusted to fit the data. The dashed line is $\sigma_\omega^p(\omega, 0)$ with $\omega_T/2\pi = 113$ MHz and $\Gamma/\omega_T = 0.78$. The dotted line is obtained by adding this term to $\sigma_{dc}^t(0, E)$. An equally good fit can be obtained for the data of Figs. 1 and 2. It is seen that the sum of these two terms closely fits the data, and thereby gives strong support to (4.3). We believe this observation to be strong evidence for an important contribution to $\sigma_\omega(\omega, 0)$ from oscillations of the pinned CDW.

C. ac-dc experiments

The experiments shown in Fig. 4 were designed to test Eq. (2.5), which gives the tunneling model prediction for the effect of a joint dc and ac excitation on $\sigma_\omega(\omega, E)$. These predictions are shown by the solid line for 30 and 80 MHz and the value used for V_1 . It is seen experimentally that the effect of V_0 is to smooth out the threshold behavior in $\sigma_\omega(\omega, E)$ and shift it to lower V_0 . In comparison, the theory predicts the persistence of a sharp threshold, which is shifted to lower V_0 , and an ω dependence to the slope above the V_0 -dependent threshold. The first feature is in qualitative disagreement with the data, the second in qualitative agreement, and the third is not tested. Although there is qualitative agreement on the second point, there is a clear quantitative disagreement. The theory indicates the rise should start at about 7 mV for 80 MHz and at about 21 mV for 30 MHz, but the experimental values are about 17 and 25 mV, respectively. The disagreement between the theory and experiment remains even when the internal excitation of Eq. (4.2) is added (with due account made for the variation of ω_T with E). It is particularly evident at 30 MHz, where the tunneling model predicts a $\sigma_\omega(\omega, E)$ which is substantially *larger* than what is observed above the threshold. We therefore see that the experiments do not

support Eq. (2.5) when both ac and dc excitations are present.

Another serious disagreement between the tunneling model and our experiments is the absence of the photon-assisted tunneling which is implied by Eq. (2.6) but not seen in Fig. 5. There, the solid line shows Eq. (2.6) using $V_1 = 2$ mV peak and the scaling relation established for this sample in Fig. 3. This disagreement presents a serious challenge to the tunneling model, which is discussed later in this section.

We have also tested the classical limit of Eq. (2.6), $\Delta I_{dc} = (V_1^2/4)d^2I/dV^2$ in measurements which are merely summarized here. Over a wide range of $V_1 < V_0$ and ω , ΔI_{dc} is about that expected of the classical limit for $\omega/2\pi < 1$ MHz. But at higher frequencies, ΔI_{dc} drops rapidly as ω is increased, until it is less than a few percent of the predicted value at $\omega \simeq \omega_T$.

Similar results have been obtained in NbSe₃ by Grüner *et al.*⁴ and by Coleman *et al.*¹⁶ for ΔI_{dc} with the application of a large amplitude ac field and the specimen biased at or below threshold. Again the expected response is observed only at very low frequencies and drops rapidly with increasing ω . For a given response, the applied ac voltage, V_1 , must be increased so as to keep V_1/ω approximately constant. As V_1/ω is increased, the response varies roughly as $(V_1/\omega)^2$.

Our conclusions with regard to the ac-dc experiments are (a) that the quantum effects predicted by the tunneling model using Tucker's formalism are absent, and (b) that only the low-frequency end of classical limit is observed experimentally.

There are several comments to be made regarding the difficulties of the models. For the classical model, it has been suggested⁴ that the significant quantity is the amplitude of the CDW oscillation in the anharmonic potential. According to this model the ac conductivity depends on the applied dc voltage. Owing to the heavily damped response, a larger V_1 is needed at larger frequencies to give the same amplitude of the oscillation as observed in the experiments. In the applied field the frequencies at the potential minima of the tilted-staircase shift with increasing field and thus change the ac response. The effect is expected to be largest near threshold, as observed. However, it may be difficult to account for the observed sharp rise $\sigma_\omega(\omega, E)$ just below E_T as shown in Fig. 4 on the basis of this model.

Although there is good agreement between experimental and theory for the predictions of the

semiconductor tunneling model for depinning of CDW's for ac and dc fields separately, the theory fails when the two are combined.

The difficulties for superimposed ac and dc fields may not come from the tunneling aspect of the theory, but from the oversimplification of the semiconductor model. It is believed that Tucker's theory should apply to this model and the shortcomings are with the model. In Tucker's theory, a quantum frequency $\hbar\omega_0 = e^*V_0$ from the dc field is combined with an ac frequency, ω . If the CDW were unpinned, the energy gained by an electron from the voltage V_0 across L would be $v_F\hbar\Delta k = e^*V_0$. This frequency is still present in the wave function for the amplitude of the tunneling electrons in the semiconductor model, but is not present for an actual CDW. The only frequency present is that associated with its motion, $\omega_d = 2k_F v_d = \omega_0 P(E)$, together with the various frequencies that are observed in narrow-band noise. The frequency ω_0 is that corresponding to the fundamental of narrow-band noise for an unpinned wave in a field V_0/L rather the actual frequency associated with the drift velocity in the pinning fields.

A theory has not yet been developed for combined ac and dc fields. Similar difficulties very likely would apply to combined high-frequency and low-frequency ac fields. It will be necessary to go beyond the semiconductor model, perhaps with a tunneling theory based on the phase model (2,1). Maki¹⁷ has worked out a theory of soliton formation by tunneling but not for motion the CDW as a whole resulting from the field.

V. CONCLUSIONS

We have reported field and frequency-dependent conductivity measurements in NbSe₃, at several temperatures with parameters chosen to test critically the semiconductor tunneling and classical models of CDW conduction. It is found that the shape of the nonlinear dc conductivity is fitted quite well by the tunneling model, and that well above threshold, its prediction of field and frequency scaling is obeyed very well. At lower fields, this scaling appears to break down. If, however, a phenomenological internal excitation of the CDW is added to rigid motion of the CDW, scaling is retained for all applied fields we have investigated. We suggest that such an excitation is present and that it forms an important contribution to the frequency-dependent conductivity near the thresh-

old for nonlinearity. When both ac and dc excitations are applied, the predictions of the tunneling model are not obeyed. In particular, photon-assisted tunneling is not observed. We conclude that although the semiconductor model adequately explains the results when only an ac or dc field is present, when both are present it oversimplifies the motion of a CDW. We find that the classical model provides a qualitative description of most aspects of the experiments, but that it does not reproduce in detail the observed response to ac or dc excitation nor the scaling seen between them. The relation of the classical model to the tunneling model is explained in the Appendix.

ACKNOWLEDGMENTS

We wish to thank N. P. Ong and R. M. Fleming for the samples used in this work, as well as P. D. Coleman for permission to mention his experimental results in advance of publication and J. R. Tucker for stimulating discussions. We are also grateful to P. M. Chaikin and T. Holstein for many discussions on CDW transport. Work on this report carried out at UCLA was supported by National Science Foundation Grant DMR 81-03085.

APPENDIX: MODELS FOR CDW PHENOMENA

Fröhlich's model¹⁸ for electron transport by moving CDW's, based on a continuum 1D model, was generalized by Allender *et al.*¹⁹ to a 1D lattice with band structure. In the ground state with no current-flow Peierls gaps open up at the Fermi surface at $\pm k_F$. When there is current flow, gaps open at the Fermi surface of the moving electrons at $-k_F + q$ and $k_F + q$. The average crystal momentum per electron is $P_e = \hbar q = m v_d$, where v_d is the drift velocity of the CDW and m is the band mass.

The phonons of the moving CDW also move at a velocity v_d , so that the charge density and potential are periodic functions, multiples of $\cos[2k_F(x - v_d t) + \phi_0]$ and various harmonics. For v_d positive, the CDW may be considered to be a state of macroscopic occupation of phonons of wave vector $2k_F$ and frequency $2k_F v_d$ with an excess of phonons moving to the right. The crystal momentum of the phonons is $P_L = M_F v_d$ per electron in the Fermi sea, where M_F is the Fröhlich mass.

For an incommensurate CDW subject to no pinning forces, the energy of the CDW system is independent of the phase, ϕ_0 . There is no energy gap to be overcome for translation of the CDW as a whole, corresponding to a finite average crystal momentum, $\hbar q$, for the ground-state electrons. The current density is $n_c e v_d$, where n_c is the density of condensed electrons, equal to the total density, n , at $T=0$ and decreasing to zero at the Peierls transition temperature, T_p , as $(T_p - T)^{1/2}$.

If there were no scattering forces that change v_d , the current would persist in time and the system would be a 1D superconductor as suggested by Fröhlich. Actual scattering is such that the conductivity in the presence of depinned CDW's is about that expected in the absence of CDW's. This may be made plausible by consideration of the following equations of motion for the momenta P_L and P_e in an electric field, E :

$$d(P_L + P_e)/dt + P_e/\tau_e = eE, \quad (\text{A1})$$

$$dP_L/dt + P_L/\tau_L = P_e/\tau_{\text{ph}}. \quad (\text{A2})$$

It is assumed that the $2k_F$ phonons gain or lose momentum only by scattering of electrons from one side of the Fermi surface to the other.

The steady-state response to a dc field, E , is $P_e = e\tau_e E$ and in equilibrium $P_L = (\tau_L/\tau_{\text{ph}})P_e = \alpha P_e$, where $\alpha = M_F/m$. The equation of motion for the electrons is then

$$dP_e/dt + P_e/\tau^* = e^*E, \quad (\text{A3})$$

where

$$\tau^*/\tau_e = e/e^* = 1 + \alpha. \quad (\text{A4})$$

For simplicity we shall assume that $\tau_{\text{ph}} \gg \tau_e$. The response to an ac field of frequency ω is then derived from

$$i\omega(P_L + P_e) + P_e/\tau_e = eE(\omega), \quad (\text{A5})$$

$$i\omega P_L + P_L/\tau_L = P_e/\tau_{\text{ph}}, \quad (\text{A6})$$

which give

$$P_e = e\tau_e E(\omega)/[1 + i\omega\tau^*(\omega)], \quad (\text{A7})$$

where

$$\tau^*(\omega) = \tau_e \left[1 + \frac{\alpha}{1 + \omega^2\tau_L^2} \right]. \quad (\text{A8})$$

Thus for $\omega\tau_L \ll 1$, $\tau^*(\omega) = \tau^* = \tau_e(1 + \alpha)$ and the conductivity is given by the usual expression, $\sigma = ne^2\tau_e/m$. For $\omega\tau_L \gg \alpha^{1/2}$, $\tau^*(\omega) = \tau_e$.

At high frequencies the electron motion becomes

decoupled from that of the ions, and the ions remain essentially at rest. If $\omega\tau_e \ll 1$, the real part of the conductivity $\sigma(\omega) = \sigma(0)$ and is independent of frequency.

The phase $\phi(x, t)$ of the CDW is equal to $2k_F(x - v_d t)$ for uniform motion. The electron density, proportional to $2k_F$, is then given by the space gradient of ϕ and the current, proportional to v_d , by the time derivative.¹⁸ The Lagrangian is²⁰

$$\frac{1}{2}N_0(\phi_t^2 - c_0^2\phi_x^2), \quad (\text{A9})$$

where in a simple model $c_0^2 = \alpha v_F^2$ is the square of the maximum soliton velocity, $N_0 = n_c \alpha m / (4k_F^2)$ and n_c is the density of electrons condensed in the CDW. Various possible ground states are available for soliton motion corresponding to different values of the drift velocity, v_d , of the CDW. Pinning forces from impurities or from commensurability tend to pin the phase of the wave and the CDW oscillates about pinning positions with a frequency ω_p . The ratio of P_L to P_e is normally fixed at the equilibrium value $P_L = \alpha P_e$. A phenomenological equation of motion per electron in the CDW is then given by²¹

$$m(d^2x/dt^2) + \Gamma(dx/dt) + \omega_p^2 x = e^*E \quad (\text{A10})$$

and the complex conductivity by (4.2). Here x represents the displacement at the center of the oscillation.

An expression similar to (4.2) is often used as an approximation (Penn²² model) to the response of a semiconductor with an energy gap $\epsilon_g = \hbar\omega_p$. A semiconductor with a gap given by the pinning frequency was used as a model for the CDW system so that the Zener theory could be used to calculate the probability of depinning by quantum tunneling across the energy gap.⁸ Such depinning allows for the possibility of the electrons becoming decoupled from the ions at high frequencies as described in the motion of unpinned CDW's previously. Since the semiclassical contribution, σ_p , does not include effects of tunneling, the two contributions to σ should be additive, at least to a first approximation. The limitations of the semiconductor model are discussed in Sec. IV.

Pinned CDW's may also be described by starting from the Lagrangian (A9) and including a phase dependent pinning potential $V(\phi_1)$ as well as a damping term.¹⁹ The equation of motion then becomes (on a per-electron basis):

$$\frac{m}{4k_F^2} \left[\frac{d^2\phi_1}{dt^2} + \Gamma \frac{d\phi_1}{dt} + \omega_p^2 V'(\phi_1) \right] = \frac{e^*E(t)}{2k_F}, \quad (\text{A11})$$

where $\phi = 2k_F(x - v_d t) + \phi_1(x, t)$ with k_F and v_d constants, ϕ_1 is a slowly varying function of x and $V'(\phi_1) = dV\phi_1/d\phi_1$ approaches ϕ_1 as $\phi_1 \rightarrow 0$.

This model gives a potential with small amplitude oscillations at the pinning frequency ω_p . The maximum of the potential barrier, depends on the form of $V(\phi_1)$ but is of the same order of magnitude as the effective barrier for electrons tunneling through the gap in the semiconductor model.

The hills and valleys of the potential are tilted by an electric field into a staircase potential. In sufficiently large fields the representative points describing the system can go over the barrier classically by thermal motion⁹ or can tunnel through⁸ at lower fields.

In the semiconductor model with a gap $\epsilon_g = 2\Delta$, the wave vector in the gap is $k_F + i\kappa$, where

$$\kappa^2 = \frac{m(\Delta^2 - \epsilon^2)}{2\hbar^2 E_F} \quad (\text{A12})$$

and ϵ is the energy measured from midgap and E_F is the Fermi energy. The effective height of the potential hill for tunneling is $V_B = \hbar^2 \kappa^2 / (2m)$. Thus the equivalent maximum barrier height (for $\epsilon = 0$) is

$$V_B = \Delta^2 / 4E_F = \epsilon_g^2 / 16E_F. \quad (\text{A13})$$

This expression is similar to that derived from a

sine-Gordon expression in the phase model

$$V(\phi) = N^{-2}(1 - \cos N\phi). \quad (\text{A14})$$

The maximum barrier height for electrons is

$$V_{\max} = m\omega_p^2 / (2k_F^2 N^2) = \epsilon_g^2 / (4E_F N^2), \quad (\text{A15})$$

which is equal to (A13) for $N = 2$. Thus the phase model and the semiconductor model are very similar and differ only in quantitative details.

In both models the acceleration of electrons in an electric field is reduced by transfer of momentum to the phonons of the CDW. In the above this has been accomplished by introducing an effective charge $e^* = e/\alpha$. One would get the same result for the tunneling probability, $P(E)$, if one introduces an effective mass $m^* = \alpha m$ and uses the ordinary electric charge, e , since only the ratio ($e/\alpha m$) enters Zener's expression for E_0 in the tunneling probability. Using m^* rather than e^* would imply using a polaron model for the electrons that constitute the CDW. There is a major difference in the magnitude of the displacement, q , of the Fermi surface for a given drift velocity, v_d . With use of e^* , $\hbar q = mv_d$ as required in Fröhlich's theory. The polaron model would give $\hbar q = (m + M_F)v_d$, a much larger value. Thus we favor the semiconductor model with $e = e^*$, although its limitations in describing CDW phenomena must be recognized.

- ¹R. M. Fleming and C. C. Grimes, *Phys. Rev. Lett.* **42**, 1423 (1979); R. M. Fleming, *Phys. Rev. B* **22**, 5606 (1980).
²G. Grüner, L. C. Tippie, J. Sanny, W. G. Clark, and N. P. Ong, *Phys. Rev. Lett.* **45**, 935 (1980).
³P. Monceau, J. Richard, and M. Renard, *Phys. Rev. Lett.* **45**, 43 (1980); M. Weger, G. Grüner, and W. G. Clark, *Solid State Commun.* **35**, 243 (1980).
⁴G. Grüner, W. G. Clark, and A. Portis, *Phys. Rev. B* (in press).
⁵J. W. Brill, N. P. Ong, J. C. Eckert, J. W. Savage, S. K. Khanna, R. B. Somoano, *Phys. Rev. B* **23**, 1517 (1981); W. W. Fuller, G. Grüner, P. M. Chaikin, and N. P. Ong, *Solid State Commun.*, in press.
⁶A. H. Thompson, A. Zettl, and G. Grüner, *Phys. Rev. Lett.* **47**, 64 (1981); G. Grüner, A. Zettl, W. G. Clark, and A. M. Thompson, *Phys. Rev. B* **23**, 6813 (1981), C. M. Jackson, A. Zettl, G. Grüner, and A. H. Thompson, *Solid State Commun.* **39**, 531 (1981).
⁷P. A. Lee and T. M. Rice, *Phys. Rev. B* **19**, 3940 (1972).
⁸J. Bardeen, *Phys. Rev. Lett.* **42**, 1498 (1979); **45**, 1978 (1980).
⁹G. Grüner, A. Zawadowski, and P. M. Chaikin, *Phys. Rev. Lett.* **46**, 511 (1981).

- ¹⁰J. R. Tucker, *IEEE J. Quant. Electron.* **15**, 1234 (1979).
¹¹J. B. Sokoloff, *Phys. Rev. B* **23**, 1992 (1981). We thank J. B. Sokoloff and R. M. Fleming, for discussing this point.
¹²S. W. Longcor and A. Portis, *Bull. Am. Phys. Soc.* **25**, 340 (1980).
¹³D. R. Penn, *Phys. Rev.* **128**, 2093 (1962).
¹⁴M. J. Rice and S. Strässler, *Solid State Commun.* **13**, 1389 (1973).
¹⁵P. A. Lee, T. M. Rice, and R. W. Anderson, *Solid State Commun.* **14**, 703 (1974).
¹⁶P. D. Coleman (unpublished).
¹⁷K. Maki, *Phys. Rev. Lett.* **35**, 46 (1977).
¹⁸H. Fröhlich, *Proc. R. Soc. London Ser. A* **233**, 296 (1954).
¹⁹D. Allender, J. W. Bray, and J. Bardeen, *Phys. Rev. B* **9**, 119 (1974).
²⁰M. J. Rice, A. B. Bishop, J. A. Krumhansl, and S. E. Trullinger, *Phys. Rev. Lett.* **36**, 432 (1976).
²¹M. J. Rice, S. Strässler, and W. R. Schneider, *One Dimensional Conductors*, Vol. 34 of *Lecture Notes in Physics*, edited by J. Ehlers, K. Hepp, R. Kippenhahn, and H. A. Weidenmüller (Springer, Berlin, 1977), pp. 282–341.